

# Atomically Precise Noble Metal Cluster-Assembled Superstructures in Water: Luminescence Enhancement and Sensing

Abhijit Nag, Papri Chakraborty, Athira Thacharon, Ganesan Paramasivam, Biswajit Mondal, Mohammad Bodiuzzaman, and Thalappil Pradeep\*

Cite This: *J. Phys. Chem. C* 2020, 124, 22298–22303

Read Online

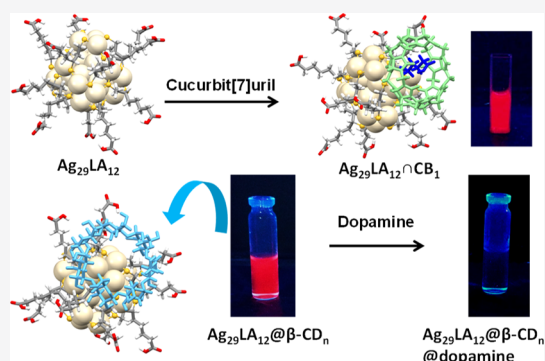
ACCESS |

Metrics & More

Article Recommendations

Supporting Information

**ABSTRACT:** We present an example of host–guest complexes of atomically precise noble metal nanoparticles with cucurbit[7]uril (CB) in water, specifically concentrating on  $\text{Ag}_{29}(\text{LA})_{12}$  (where LA is  $\alpha$ -lipoic acid), a well-known red luminescent silver cluster. Such host–guest interactions resulted in enhanced luminescence of about 1.25 times for the modified system, compared to the parent cluster. We extended our study to cyclodextrins (CDs), where about 1.5 times enhanced luminescence was estimated compared to the parent cluster. The formation of supramolecular complexes was confirmed using high-resolution electrospray ionization mass spectrometry (HRESI MS) and nuclear magnetic resonance spectroscopy. Molecular docking and density functional theory calculations supported our experimental results and showed that while CB formed inclusion complexes by encapsulation of one of the LA ligands of the cluster, CD formed supramolecular adducts by interaction with the cavity built by the ligands on the cluster surface. The complexation was favored by geometrical compatibility. Consequently, these superstructures are labeled as  $\text{Ag}_{29}\text{LA}_{12}\cap\text{CB}_n$  and  $\text{Ag}_{29}\text{LA}_{12}\text{@CD}_n$  ( $n = 1-3$ ), where  $\cap$  and  $\text{@}$  indicate the inclusion complex and supramolecular adduct, respectively. Solution-phase  $\text{Ag}_{29}\text{LA}_{12}\text{@CD}_n$  complexes were employed to detect dopamine (10 nM). Luminescent  $\text{Ag}_{29}\text{LA}_{12}\text{@CD}_n$  and  $\text{Ag}_{29}\text{LA}_{12}\cap\text{CB}_n$  complexes in water could be potential candidates for organic pollutant sensing and biomedical applications.



## INTRODUCTION

Noble metal nanoclusters (NMCs) have emerged as new functional nanomaterials<sup>1–3</sup> because of their wide range of applications including biomedical imaging,<sup>4</sup> sensing,<sup>5</sup> catalysis,<sup>6,7</sup> energy conversion,<sup>8</sup> and so forth. Various properties of NMCs like catalysis, chirality, and photoluminescence (PL) are controlled by not only the central metal core but also the ligands.<sup>2,9,10</sup> Diverse organic ligands including thiolates,<sup>11–13</sup> phosphines,<sup>14–17</sup> and alkynes<sup>18,19</sup> have been used for the synthesis of NMCs.

Supramolecular chemistry involves chemical methods to build complex structures from simple molecular building blocks via noncovalent interactions. Noncovalent interactions include ion–ion, hydrogen bonding,  $\pi$ – $\pi$  stacking, and van der Waals (vdWs) interactions.<sup>20,21</sup> Such interactions of nanoparticles resulted in self-assembled superstructures.<sup>22</sup> As the nanoclusters are protected by organic ligands, supramolecular complexation is possible for NMCs also.<sup>20</sup> Cyclodextrins (CDs) and cucurbit[7]uril (CB) were used in supramolecular chemistry because of their encapsulation activity.<sup>23</sup> Recently, Mathew et al. reported the host–guest complexation of  $[\text{Au}_{25}(\text{SBB})_{18}]^-$  with  $\beta$ -CD.<sup>24</sup> Moussawi et al. synthesized and crystallized a supramolecular hybrid complex of a polyoxometalate  $[\text{P}_2\text{W}_{18}\text{O}_{62}]^{6-}$ ,  $\gamma$ -CD, and  $[\text{Ta}_6\text{Br}_{12}(\text{H}_2\text{O})_6]^{2+}$ ,

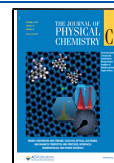
where CD acted as a linker between polyoxometalate and the cluster.<sup>25</sup> Recently, our group reported isomerism in  $\text{Ag}_{29}\text{BDT}_{12}\cap\beta\text{-CD}_n$  (where BDT is 1,3-benzenedithiol;  $n = 2-4$ ) complexes.<sup>26</sup> The supramolecular complexes of  $[\text{Ag}_{29}(\text{BDT})_{12}]^{3-}$  with fullerenes ( $\text{C}_{60}$  and  $\text{C}_{70}$ ) were also studied.<sup>27</sup> The crystal structure of the supramolecular complexes of crown ethers with  $\text{Ag}_{29}\text{BDT}_{12}$  was resolved, and the driving forces for such complexation were seen to be noncovalent interactions.<sup>28</sup> Such supramolecular interactions could assemble them in crystalline superstructures because of the strong noncovalent interactions. CB belongs to a family of host molecules which could form assemblies with NMCs. The supramolecular complexation of luminescent clusters with CDs and CB in water could be highly useful for biomedical applications.

A supramolecular adduct is one in which molecular interactions bring two species together. An inclusion complex

Received: July 28, 2020

Revised: September 16, 2020

Published: September 16, 2020



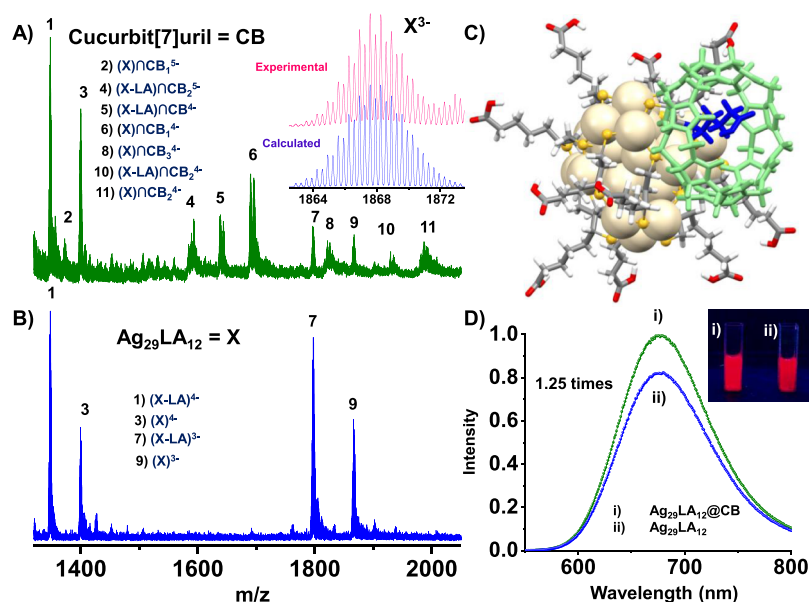


**Figure 1.** Full-range HRESI MS spectra of  $[\text{Ag}_{29}(\text{LA})_{12} \cap \text{CB}_n]$  complexes, where  $n = 1-3$  (A) and  $\text{Ag}_{29}(\text{LA})_{12}$  (B). Relative peak intensities of the isotopologues of  $\text{Ag}_{29}(\text{LA})_{12}^{3-}$  are presented in the inset of (A). Assignments of the peaks are provided in the inset of (A,B) with numbering, where  $X = \text{Ag}_{29}(\text{LA})_{12}$ . (C) Schematic representation of  $[\text{Ag}_{29}(\text{LA})_{12} \cap \text{CB}_n]$  for  $n = 1$ . Color codes: silver, light yellowish gray; sulfur, yellow; carbon, gray; oxygen, red. Encapsulated LA inside CB is in blue. CB is presented in light green color. (D) PL spectra of  $[\text{Ag}_{29}(\text{LA})_{12} \cap \text{CB}_n]$  complexes (i) and pure cluster (ii). Photographs of the solution of  $[\text{Ag}_{29}(\text{LA})_{12} \cap \text{CB}_n]$  complexes (i) and  $[\text{Ag}_{29}(\text{LA})_{12}]$  (ii) under UV light are shown in the inset of (D).

is a specific category of supramolecular adducts in which a molecule having a cavity hosts a guest molecule. We can simply term both of them as supramolecular complexes, as all inclusion complexes are supramolecular adducts, although all supramolecular adducts are not inclusion complexes.

Here, we report the supramolecular complexation of  $\text{Ag}_{29}\text{LA}_{12}$  (where LA is  $\alpha$ -lipoic acid) with CB and CDs in water. Such noncovalent interactions resulted in enhanced luminescence of about 1.5 and 1.25 times for  $\beta$ -CD and CB, respectively, compared to the parent cluster. We used mass spectrometry (MS) along with critical inputs from nuclear magnetic resonance (NMR) spectroscopy and computational studies to characterize  $\text{Ag}_{29}\text{LA}_{12}@\text{CD}_n$  and  $\text{Ag}_{29}\text{LA}_{12} \cap \text{CB}_n$  ( $n = 1-3$ ) complexes, which were stabilized mainly by vdWs and hydrogen-bonding interactions. Density functional theory (DFT) studies suggested that CB encapsulated one of the LA ligands, whereas CD interacted with a cavity on the cluster surface created by the ligands. Highly luminescent  $\text{Ag}_{29}\text{LA}_{12}@\beta\text{-CD}_n$  complexes were utilized to detect dopamine selectively in solution at very low concentrations (10 nM). Dopamine is one of the main neurotransmitters of both peripheral and central nervous systems, and a change of its concentration from the normal range has been connected with diseases such as Alzheimer's and Parkinson's diseases. Hence, the development of a simple method to detect dopamine is noteworthy. There have been a few methods introduced earlier to sense dopamine.<sup>29,30</sup>

## EXPERIMENTAL SECTION

**Chemicals and Materials.**  $\text{AgNO}_3$ ,  $\text{NaBH}_4$ , ( $\pm$ )- $\alpha$ -lipoic acid, CDs ( $\alpha$ ,  $\beta$ , and  $\gamma$ ), CB,  $\text{D}_2\text{O}$ , phenylalanine, ascorbic acid, glucose, dopamine, and methanol were obtained from Sigma-Aldrich. Butanol and  $\text{H}_2\text{O}_2$  were obtained from Rankem. Milli-Q quality water was used throughout the experiment.

**Synthesis of  $[\text{Ag}_{29}(\text{LA})_{12}@\text{CD}_n]$  Complexes.** About 19 mg LA and 7 mg  $\text{NaBH}_4$  were mixed in 14 mL of water in a glass bottle. This mixture was stirred (using a magnetic pellet) until it became a clear solution. Next, about 700  $\mu\text{L}$  of 25 mM  $\text{AgNO}_3$  solution was added (the solution became turbid), followed by 10 mg  $\text{NaBH}_4$  in 2 mL of water. The bottle was covered with an aluminum foil to minimize the exposure of the clusters to light. After 4–5 h, the clusters were formed. About 10 mg of CD was added to the cluster solution, and the reaction was continued for about 2 h. The reaction was done at room temperature under continuous magnetic stirring. The samples were kept in a fridge after covering the bottle with an aluminum foil. The clusters were purified with BuOH by mixing 300  $\mu\text{L}$  of clusters, 400  $\mu\text{L}$  of BuOH, and 100  $\mu\text{L}$  of methanol in a 2 mL vial. The mixture was centrifuged to accelerate phase separation, and the upper colorless organic layer was removed. This was repeated until the clusters were sedimented. Typically, three to five extractions with BuOH were required. A gum-like material was obtained after purification.

**Synthesis of  $[\text{Ag}_{29}(\text{LA})_{12} \cap \text{CB}_n]$  Complexes.** About 2 mg of CB was dissolved in 2 mL of Milli-Q water. Next, about 100  $\mu\text{L}$  of this solution was added to the purified cluster solution at the required concentration.

**Instrumentation. Electro Spray Ionization MS.** All MS measurements were performed using a Waters Synapt G2Si high-definition mass spectrometer equipped with electro spray ionization (ESI) and ion mobility separation. All measurements were carried out in the negative ion mode. The instrument was calibrated using NaI as the calibrant. The typical experimental parameters were: desolvation gas temperature, 150  $^\circ\text{C}$ ; source temperature, 100  $^\circ\text{C}$ ; desolvation gas flow, 400 L/h; capillary voltage, 3 kV; sample cone, 0 V; source offset, 0 V; trap collision energy, 2 V; and trap gas flow, 2 mL/min. The sample was infused at a flow rate of 30  $\mu\text{L}/\text{min}$ .

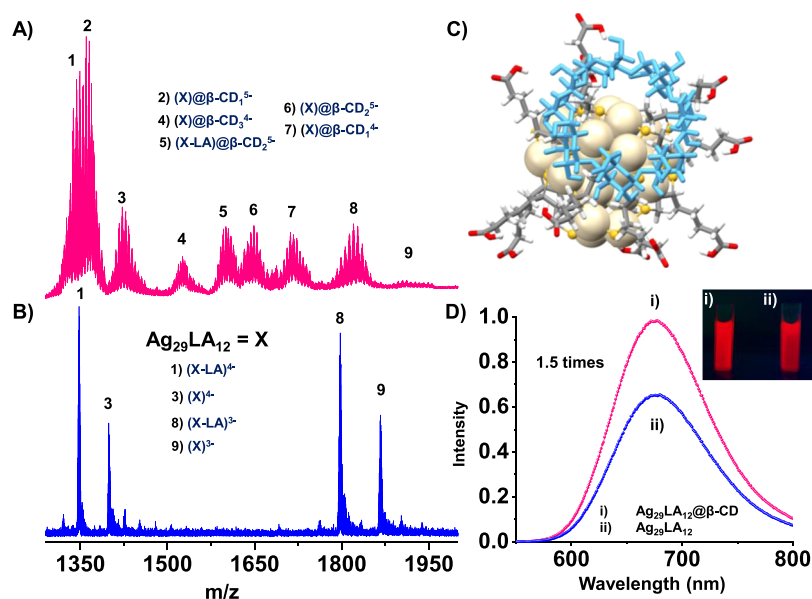


**Figure 2.** HRESI MS of  $[\text{Ag}_{29}(\text{LA})_{12}@\beta\text{-CD}_n]$  complexes, where  $n = 1-3$  (A) and  $\text{Ag}_{29}(\text{LA})_{12}$  (B). Assignments of the peaks are provided in the inset of (A,B) with numbering, where  $X = \text{Ag}_{29}(\text{LA})_{12}$ . Branching of peaks appeared because of the presence of Na adducts.  $[\text{X}\cap\text{CD}_3]^{4-}$  (peak 4) is lighter than  $[\text{X}\cap\text{CD}_1]^{4-}$  (peak 7) in (A) because of Na attachments. (C) Schematic representation of  $[\text{Ag}_{29}(\text{LA})_{12}@\beta\text{-CD}_n]$  for  $n = 1$ . Color codes: silver, light yellowish gray; sulfur, yellow; carbon, gray; oxygen, red. CD is presented in light blue color. (D) PL spectra of  $[\text{Ag}_{29}(\text{LA})_{12}@\beta\text{-CD}_n]$  complexes (i) and pure cluster (ii). Photographs of the solution of  $[\text{Ag}_{29}(\text{LA})_{12}@\beta\text{-CD}_n]$  complexes (i) and  $[\text{Ag}_{29}(\text{LA})_{12}]$  (ii) under UV light are shown in the inset of (D).

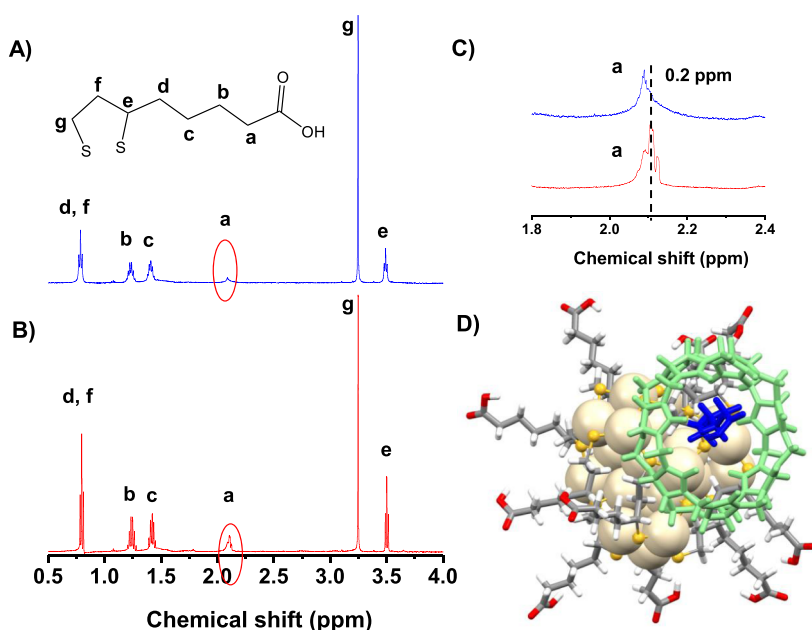


**Figure 3.** <sup>1</sup>H NMR spectra of  $[\text{Ag}_{29}(\text{LA})_{12}@\text{CB}_n]$  (A) and  $\text{Ag}_{29}(\text{LA})_{12}$  (B). Assignments of the peaks are provided. (C) Zoomed-in view of the peak “a” from (A,B), which shows a significant change after the supramolecular complexation with  $\sim 0.2$  ppm chemical shift. (D) DFT-optimized structure of  $[\text{Ag}_{29}(\text{LA})_{12}@\text{CB}_1]$ . The color codes remain the same as in Figure 1. Encapsulated LA and CB are shown in blue and light green, respectively.

More details on instrumentation are presented in the [Supporting Information](#). Computational details are also presented in the [Supporting Information](#).

## RESULTS AND DISCUSSION

In the discussion presented below, supramolecular complexes are designated as  $\text{Ag}_{29}(\text{LA})_{12}@\text{CB}_n$  and  $\text{Ag}_{29}(\text{LA})_{12}@\text{CD}_n$ , although the exact nature of complexation will be confirmed only by a combination of studies.

**Characterization of  $[\text{Ag}_{29}(\text{LA})_{12}@\text{CB}_n]$  Complexes.** The supramolecular complexes of  $\text{Ag}_{29}(\text{LA})_{12}$  with CB were confirmed using high-resolution ESI MS (HRESI MS) (Figure 1A). ESI MS spectra of  $[\text{Ag}_{29}(\text{LA})_{12}@\text{CB}_n]$  and  $[\text{Ag}_{29}(\text{LA})_{12}]$  are shown in Figure 1A,B. The assignments of the peaks are given in the inset of Figure 1A with appropriate numbering. Peaks 2, 6, 8, and 11 correspond to  $(\text{X})\cap\text{CB}_1^{5-}$ ,  $(\text{X})\cap\text{CB}_1^{4-}$ ,  $(\text{X})\cap\text{CB}_3^{4-}$ , and  $(\text{X})\cap\text{CB}_2^{4-}$ , respectively, where  $X = \text{Ag}_{29}(\text{LA})_{12}$  (Figure 1B). Loss of ligands and CB was observed

in the case of  $[\text{Ag}_{29}(\text{LA})_{12}\cap\text{CB}_n]$  ( $n = 1-3$ ), which could be due to the voltages applied during ESI MS measurements. The loss of ligands was observed for the parent cluster also. Various charge states of the complexes were detected because of the presence of carboxylic acid groups on the cluster, which was also previously seen in the case of  $\text{Ag}_{29}\text{LA}_{12}$ <sup>31</sup> and  $\text{Ag}_{11}(\text{SG})_7$ <sup>32</sup>  $[\text{X}\cap\text{CB}_3]^{4-}$  (peak 8) is lighter than  $[\text{X}\cap\text{CB}_2]^{4-}$  (peak 11) in Figure 1A. This is due to the number of  $\text{Na}^+$  attachments. Moreover, the supramolecular interactions of  $[\text{Ag}_{29}(\text{LA})_{12}\cap\text{CB}_n]$  complexes resulted in 1.25 times enhancement in luminescence, compared to the parent cluster (Figure 1D). However, the emission maximum of  $[\text{Ag}_{29}(\text{LA})_{12}\cap\text{CB}_n]$  complexes ( $\sim 680$  nm) was almost the same as that of  $\text{Ag}_{29}(\text{LA})_{12}$ . The emission spectra of the cluster and its supramolecular complexes with CB are provided in Figure 1D. Photographs of the solution of  $[\text{Ag}_{29}(\text{LA})_{12}\cap\text{CB}_n]$  complexes and  $[\text{Ag}_{29}(\text{LA})_{12}]$  under UV light are shown in the inset of Figure 1D. The optical absorption features showed similar nature to that of the cluster, with a slightly decreasing absorption, as shown in Figure S2.

**Characterization of  $[\text{Ag}_{29}(\text{LA})_{12}\text{@}\beta\text{-CD}_n]$  Complexes.** The as-synthesized  $[\text{Ag}_{29}(\text{LA})_{12}\text{@}\beta\text{-CD}_n]$  ( $n = 1-3$ ) complexes were characterized using HRESI MS. ESI MS spectra of  $[\text{Ag}_{29}(\text{LA})_{12}\text{@}\beta\text{-CD}_n]$  ( $n = 1-3$ ) complexes are provided in Figure 2A. The assignments of the peaks are mentioned in the inset of Figure 2A,B. Peaks 2, 4, 6, and 7 represent  $(\text{X})\text{@}\beta\text{-CD}_1^{5-}$ ,  $(\text{X})\text{@}\beta\text{-CD}_3^{4-}$ ,  $(\text{X})\text{@}\beta\text{-CD}_2^{5-}$ , and  $(\text{X})\text{@}\beta\text{-CD}_1^{4-}$ , respectively, where  $\text{X} = \text{Ag}_{29}(\text{LA})_{12}$ . The ESI MS spectrum of  $\text{Ag}_{29}(\text{LA})_{12}$  is provided in Figure 2B. The loss of ligands and CDs was similar in nature with the  $[\text{Ag}_{29}(\text{LA})_{12}\cap\text{CB}_n]$  ( $n = 1-3$ ) complexes. Moreover, various charge states of the complexes were observed in this case also. In the case of  $\alpha$  and  $\gamma$ -CD, similar types of adduct formation were confirmed using HRESI MS. The ESI MS spectra of  $[\text{Ag}_{29}(\text{LA})_{12}\text{@}\alpha\text{-CD}_n]$  and  $[\text{Ag}_{29}(\text{LA})_{12}\text{@}\gamma\text{-CD}_n]$  complexes are provided in Figures S3 and S4, respectively. After forming such supramolecular adducts,  $[\text{Ag}_{29}(\text{LA})_{12}\text{@}\beta\text{-CD}_n]$  complexes became more stable compared to only  $\text{Ag}_{29}(\text{LA})_{12}$ .  $[\text{Ag}_{29}(\text{LA})_{12}\text{@}\beta\text{-CD}_n]$  complexes were 1.5 times more luminescent compared to the parent cluster. The emission spectra of  $\text{Ag}_{29}(\text{LA})_{12}$  and its CD complexes are provided in Figure 2D. The UV-vis features of  $[\text{Ag}_{29}(\text{LA})_{12}\text{@}\beta\text{-CD}_n]$  and  $\text{Ag}_{29}(\text{LA})_{12}$  were almost similar, which indicated that the electronic structure of the cluster was unaltered by CD complexation (Figure S5). Photographs of the solution of  $[\text{Ag}_{29}(\text{LA})_{12}\text{@}\beta\text{-CD}_n]$  complexes and  $[\text{Ag}_{29}(\text{LA})_{12}]$  under UV light are provided in the inset of Figure 2D.

**NMR Study.** Solution-phase NMR studies were performed in order to understand the interactions between the cluster and CB. The  $^1\text{H}$  NMR spectra for  $[\text{Ag}_{29}(\text{LA})_{12}\cap\text{CB}_n]$  and  $\text{Ag}_{29}(\text{LA})_{12}$  cluster are shown in Figure 3A,B. Zoomed in views of peak “a” from Figure 3A,B are shown in Figure 3C, where a triplet peak was converted to a singlet peak along with  $\sim 0.2$  ppm upfield chemical shift because of the change in the environment of the proton of LA after supramolecular complexation. This supported the existence of supramolecular interactions in the solution phase. Similarly,  $^1\text{H}$  NMR for  $[\text{Ag}_{29}(\text{LA})_{12}\text{@}\beta\text{-CD}_n]$  complexes was also performed. The  $^1\text{H}$  NMR spectra for  $[\text{Ag}_{29}(\text{LA})_{12}\text{@}\beta\text{-CD}_n]$  and  $\text{Ag}_{29}(\text{LA})_{12}$  are shown in Figure S6A,B. Because of the strong interactions, almost all the peaks,  $\text{H}_1\text{--H}_6$ , showed an upfield shift.  $\text{H}_4$  of the  $\beta\text{-CD}$  peak overlapped with the “e” peak of LA. As a result, the overall intensity of the peak increased.

### Computational Study to Understand the Structures of $[\text{Ag}_{29}(\text{LA})_{12}\cap\text{CB}_n]$ and $[\text{Ag}_{29}(\text{LA})_{12}\text{@}\beta\text{-CD}_n]$ Complexes.

Lopez et al. reported that the core structure of  $\text{Ag}_{29}(\text{LA})_{12}$  is analogous to that of  $\text{Ag}_{29}(\text{BDT})_{12}$ .<sup>33</sup> Using this reported DFT method, we optimized the structure of  $\text{Ag}_{29}(\text{LA})_{12}^{3-}$ . We performed molecular docking, followed by DFT optimization, to understand the structures of  $[\text{Ag}_{29}(\text{LA})_{12}\cap\text{CB}_n]$  and  $[\text{Ag}_{29}(\text{LA})_{12}\text{@}\beta\text{-CD}_n]$  complexes. Molecular docking was carried out in order to get the lowest minimum geometry for  $[\text{Ag}_{29}(\text{LA})_{12}\cap\text{CB}_1]$  and  $[\text{Ag}_{29}(\text{LA})_{12}\text{@}\beta\text{-CD}_1]$ . We used  $\text{Ag}_{29}(\text{LA})_{12}$  as the “ligand” and supramolecular agents (CB and  $\beta\text{-CD}$ ) as the “receptor” molecules. DFT was carried out after obtaining the lowest energy structure from the docking study. The DFT-optimized structure of  $[\text{Ag}_{29}(\text{LA})_{12}\cap\text{CB}_1]$  is shown in Figures 3D and S7, where one CB molecule (light green) encapsulated one LA ligand (blue) of  $\text{Ag}_{29}(\text{LA})_{12}$ . The binding energy value was  $-12.58$  kcal/mol. The optimized structure of  $[\text{Ag}_{29}(\text{LA})_{12}\cap\text{CB}_1]$  revealed that vdWs and dipole–dipole interactions were responsible for such a type of complexation. Similarly, we optimized the structure of  $[\text{Ag}_{29}(\text{LA})_{12}\text{@}\beta\text{-CD}_1]$  using DFT. The optimized structure of this system is shown in Figure S8. Here, LA ligands anchored on the cluster surface formed a cavity, into which the CD molecule (light blue) could fit. The wider rim of CD interacted with the LA ligands of this cavity. The binding energy value was  $-70.01$  kcal/mol. vdW and hydrogen-bonding interactions were the primary reasons for such supramolecular complexation. We also obtained the structures of  $[\text{Ag}_{29}(\text{LA})_{12}\cap\text{CB}_2]$  and  $[\text{Ag}_{29}(\text{LA})_{12}\text{@}\beta\text{-CD}_2]$  complexes using molecular docking and DFT optimization. The structures and binding energies of  $[\text{Ag}_{29}(\text{LA})_{12}\cap\text{CB}_2]$  and  $[\text{Ag}_{29}(\text{LA})_{12}\text{@}\beta\text{-CD}_2]$  complexes are shown in Figures S9 and S10, respectively. Various possibilities of binding of CB and CD with the cluster were examined. From these calculations, it was confirmed that CB formed inclusion complexes with  $\text{Ag}_{29}(\text{LA})_{12}$ , whereas CD formed simple supramolecular adducts.

**Dopamine Sensing.** Dopamine has several important functions in brain and body. Previously, various methods such as electrochemical, calorimetric, fluorescence, and so forth were used for sensing this molecule, and a summary of such studies is provided in Table S1. As the cavity of the CD in the complexes is free to encapsulate other molecules, we used  $[\text{Ag}_{29}(\text{LA})_{12}\text{@}\beta\text{-CD}_n]$  to sense dopamine. The luminescence of  $[\text{Ag}_{29}(\text{LA})_{12}\text{@}\beta\text{-CD}_n]$  was quenched upon the addition of dopamine, at a concentration of 1 mM (Figure 4A).  $[\text{Ag}_{29}(\text{LA})_{12}\text{@}\beta\text{-CD}_n]$  did not respond to other related species like glucose,  $\text{H}_2\text{O}_2$ , phenylalanine, and ascorbic acid at a concentration of 1 mM (Figure 4A). These species tested are likely to exist in such situations. Photographs of the solutions of  $[\text{Ag}_{29}(\text{LA})_{12}\text{@}\beta\text{-CD}_n]$  before and after the addition of glucose,  $\text{H}_2\text{O}_2$ , phenylalanine, dopamine, and ascorbic acid are shown in Figure 4B. The vacant cavity of CD could encapsulate dopamine molecules, leading to such quenching. PL intensity decreased upon increasing the dopamine concentration in solution (Figure S11A). About 10 nM dopamine solution was detected by this method (Figure S11A). Comparison of our data with the literature is provided in Table S1. Previously, CD-based gold nanoparticles were used to sense dopamine.<sup>34</sup> Fluorescent gold nanoclusters were also used for the selective detection of dopamine.<sup>35</sup> Here, luminescent supramolecular complexes of atomically precise silver cluster were utilized to detect dopamine in water. This is the first example of dopamine sensing using supramolecular

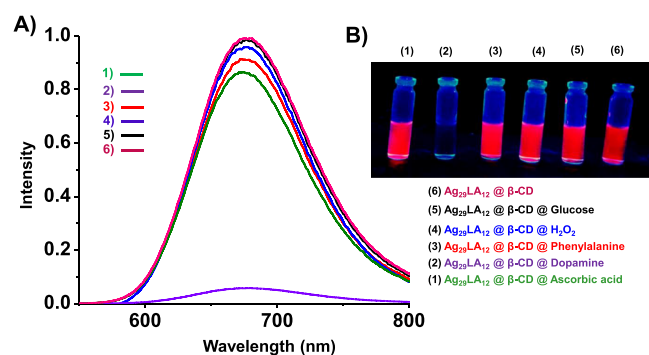


**Figure 4.** (A) PL spectra of  $[Ag_{29}(LA)_{12}@\beta-CD_n]$  complexes before (6) and after the addition of glucose (5),  $H_2O_2$  (4), phenylalanine (3), dopamine (2), and ascorbic acid (1) and (B) their corresponding photographs. The final concentration of all above species was 1 mM. The color of the species in (A,B) is kept the same in the PL spectra.

complexes of atomically precise clusters. Quenching data at different concentrations of dopamine are provided in Figure S11A. The plot between PL quenching efficiency and dopamine concentration shows a linear relationship (Figure S11B).

Regarding other implications of these structures, we suggest that their isolation in the solid state can result in new classes of cluster-assembled solids. Such cluster-assembled solids are likely to be functional materials. The vacant cavity of  $\beta$ -CD in  $[Ag_{29}(LA)_{12}@\beta-CD_n]$  complexes could be utilized for sensing organic pollutants in air, besides their use in drug delivery and bioimaging, as the cluster is likely to be biocompatible. Although these are only suggestions at the moment, we believe that such supramolecular complexes presented here may bring new aspects into the expanding science of NMCs.

## CONCLUSIONS

In summary, we showed the formation of supramolecular complexes of  $Ag_{29}(LA)_{12}$  with CB and CDs. Noncovalent interactions enhanced the luminescence of the cluster. The formation of  $Ag_{29}LA_{12}@CD_n$  and  $Ag_{29}LA_{12}\cap CB_n$  ( $n = 1-3$ ) complexes was characterized using HRESI MS and NMR. Molecular docking and DFT calculations supported the experimental results. Supramolecular complexes of  $Ag_{29}LA_{12}@\beta-CD_n$  were used to detect dopamine in solution at a limit of 10 nM with high selectivity. Host-guest complexation could be observed for other clusters also depending on the symmetry, orientation, and geometry of the ligands surrounding the cluster.

## ASSOCIATED CONTENT

### Supporting Information

The Supporting Information is available free of charge at <https://pubs.acs.org/doi/10.1021/acs.jpcc.0c06770>.

Experimental and computational details; ESI MS and UV-vis spectra of  $[Ag_{29}(LA)_{12}]$ ; UV-vis spectra of  $[Ag_{29}(LA)_{12}\cap CB_n]$  and  $Ag_{29}(LA)_{12}$ ; HRESI MS spectra of  $[Ag_{29}(LA)_{12}@\alpha-CD_n]$  and  $[Ag_{29}(LA)_{12}@\gamma-CD_n]$ ; UV-vis spectrum of  $[Ag_{29}(LA)_{12}@\beta-CD_n]$ ;  $^1H$  NMR of  $[Ag_{29}(LA)_{12}@\beta-CD_n]$  and  $Ag_{29}(LA)_{12}$ ; DFT-optimized structures of  $[Ag_{29}(LA)_{12}\cap CB_1]$ ,  $[Ag_{29}(LA)_{12}@\beta-CD_1]$ ,  $[Ag_{29}(LA)_{12}\cap CB_2]$ , and  $[Ag_{29}(LA)_{12}@\beta-CD_2]$ ; PL spectra of  $[Ag_{29}(LA)_{12}@\beta-CD_n]$ ; and coordinates of the structures (PDF)

## AUTHOR INFORMATION

### Corresponding Author

Thalappil Pradeep – DST Unit of Nanoscience and Thematic Unit of Excellence, Department of Chemistry, Indian Institute of Technology Madras, Chennai 600036, India; [orcid.org/0000-0003-3174-534X](https://orcid.org/0000-0003-3174-534X); Email: [pradeep@iitm.ac.in](mailto:pradeep@iitm.ac.in); Fax: +91-44 2257-0545

### Authors

Abhijit Nag – DST Unit of Nanoscience and Thematic Unit of Excellence, Department of Chemistry, Indian Institute of Technology Madras, Chennai 600036, India

Papri Chakraborty – DST Unit of Nanoscience and Thematic Unit of Excellence, Department of Chemistry, Indian Institute of Technology Madras, Chennai 600036, India

Athira Thacharon – DST Unit of Nanoscience and Thematic Unit of Excellence, Department of Chemistry, Indian Institute of Technology Madras, Chennai 600036, India

Ganesan Paramasivam – DST Unit of Nanoscience and Thematic Unit of Excellence, Department of Chemistry, Indian Institute of Technology Madras, Chennai 600036, India

Biswajit Mondal – DST Unit of Nanoscience and Thematic Unit of Excellence, Department of Chemistry, Indian Institute of Technology Madras, Chennai 600036, India

Mohammad Bodiuzzaman – DST Unit of Nanoscience and Thematic Unit of Excellence, Department of Chemistry, Indian Institute of Technology Madras, Chennai 600036, India

Complete contact information is available at:

<https://pubs.acs.org/10.1021/acs.jpcc.0c06770>

### Author Contributions

A.N. designed and conducted all experiments. P.C., A.T., and A.N. synthesized the clusters and carried out the ESI MS measurements. G.P. carried out the DFT calculations. A.N. carried out the molecular docking simulations. The whole project was supervised by T.P. The manuscript was written through contributions of all authors. All authors have given approval to the final version of the manuscript.

### Notes

The authors declare no competing financial interest.

## ACKNOWLEDGMENTS

The authors thank the Department of Science and Technology, Government of India, for constantly supporting our research program on nanomaterials. A.N. and B.M. thank IIT Madras for doctoral fellowships. P.C. thanks the Council of Scientific and Industrial Research (CSIR) for her research fellowship. G.P. thanks IIT Madras for an Institute Postdoctoral fellowship. M.B. thanks University Grants Commission (UGC) for his research fellowship.

## ABBREVIATIONS

CB, cucurbit[7]uril; CDs, cyclodextrins; HRESI MS, high-resolution electrospray ionization mass spectrometry; NMR, nuclear magnetic resonance; DFT, density functional theory; NMCs, noble metal nanoclusters; vdWs, van der Waals; SBB, 4-(*t*-butyl)benzyl mercaptan

## REFERENCES

(1) Chakraborty, I.; Pradeep, T. Atomically Precise Clusters of Noble Metals: Emerging Link between Atoms and Nanoparticles. *Chem. Rev.* **2017**, *117*, 8208–8271.

- (2) Jin, R.; Zeng, C.; Zhou, M.; Chen, Y. Atomically Precise Colloidal Metal Nanoclusters and Nanoparticles: Fundamentals and Opportunities. *Chem. Rev.* **2016**, *116*, 10346–10413.
- (3) Chakraborty, P.; Pradeep, T. The Emerging Interface of Mass Spectrometry with Materials. *NPG Asia Mater.* **2019**, *11*, 48.
- (4) Song, X.-R.; Goswami, N.; Yang, H.-H.; Xie, J. Functionalization of Metal Nanoclusters for Biomedical Applications. *Analyst* **2016**, *141*, 3126–3140.
- (5) Yuan, X.; Luo, Z.; Yu, Y.; Yao, Q.; Xie, J. Luminescent Noble Metal Nanoclusters as an Emerging Optical Probe for Sensor Development. *Chem.—Asian J.* **2013**, *8*, 858–871.
- (6) Kurashige, W.; Niihori, Y.; Sharma, S.; Negishi, Y. Precise Synthesis, Functionalization and Application of Thiolate-Protected Gold Clusters. *Coord. Chem. Rev.* **2016**, *320–321*, 238–250.
- (7) Yamazoe, S.; Koyasu, K.; Tsukuda, T. Nonscalable Oxidation Catalysis of Gold Clusters. *Acc. Chem. Res.* **2014**, *47*, 816–824.
- (8) Mathew, A.; Pradeep, T. Noble Metal Clusters: Applications in Energy, Environment, and Biology. *Part. Part. Syst. Charact.* **2014**, *31*, 1017–1053.
- (9) Kang, X.; Zhu, M. Tailoring the Photoluminescence of Atomically Precise Nanoclusters. *Chem. Soc. Rev.* **2019**, *48*, 2422–2457.
- (10) Knoppe, S.; Bürgi, T. Chirality in Thiolate-Protected Gold Clusters. *Acc. Chem. Res.* **2014**, *47*, 1318–1326.
- (11) Joshi, C. P.; Bootharaju, M. S.; Alhilaly, M. J.; Bakr, O. M.  $[\text{Ag}_{25}(\text{SR})_{18}]^-$ : The “Golden” Silver Nanoparticle. *J. Am. Chem. Soc.* **2015**, *137*, 11578–11581.
- (12) Zhu, M.; Aikens, C. M.; Hollander, F. J.; Schatz, G. C.; Jin, R. Correlating the Crystal Structure of A Thiol-Protected  $\text{Au}_{25}$  Cluster and Optical Properties. *J. Am. Chem. Soc.* **2008**, *130*, 5883–5885.
- (13) Heaven, M. W.; Dass, A.; White, P. S.; Holt, K. M.; Murray, R. W. Crystal Structure of the Gold Nanoparticle  $[\text{N}(\text{C}_8\text{H}_{17})_4]^-[\text{Au}_{25}(\text{SCH}_2\text{CH}_2\text{Ph})_{18}]^-$ . *J. Am. Chem. Soc.* **2008**, *130*, 3754–3755.
- (14) AbdulHalim, L. G.; Bootharaju, M. S.; Tang, Q.; Del Gobbo, S.; AbdulHalim, R. G.; Eddaoudi, M.; Jiang, D.-e.; Bakr, O. M.  $\text{Ag}_{29}(\text{BDT})_{12}(\text{TPP})_4$ : A Tetravalent Nanocluster. *J. Am. Chem. Soc.* **2015**, *137*, 11970–11975.
- (15) Nag, A.; Chakraborty, P.; Bodiuzzaman, M.; Ahuja, T.; Antharjanam, S.; Pradeep, T. Polymorphism of  $\text{Ag}_{29}(\text{BDT})_{12}(\text{TPP})_4^{3-}$  Cluster: Interactions of Secondary Ligands and Their Effect on Solid State Luminescence. *Nanoscale* **2018**, *10*, 9851–9855.
- (16) Bodiuzzaman, M.; Ghosh, A.; Sugi, K. S.; Nag, A.; Khatun, E.; Varghese, B.; Paramasivam, G.; Antharjanam, S.; Natarajan, G.; Pradeep, T. Camouflaging Structural Diversity: Co-crystallization of Two Different Nanoparticles Having Different Cores But the Same Shell. *Angew. Chem., Int. Ed.* **2019**, *58*, 189–194.
- (17) Ghosh, A.; Bodiuzzaman, M.; Nag, A.; Jash, M.; Baksi, A.; Pradeep, T. Sequential Dihydrogen Desorption from Hydride-Protected Atomically Precise Silver Clusters and the Formation of Naked Clusters in the Gas Phase. *ACS Nano* **2017**, *11*, 11145–11151.
- (18) Tomihara, R.; Hirata, K.; Yamamoto, H.; Takano, S.; Koyasu, K.; Tsukuda, T. Collision-Induced Dissociation of Undecagold Clusters Protected by Mixed Ligands  $[\text{Au}_{11}(\text{PPh}_3)_8\text{X}_2]^+$  ( $\text{X} = \text{Cl}, \text{C}\equiv\text{CPh}$ ). *ACS Omega* **2018**, *3*, 6237–6242.
- (19) Maity, P.; Tsunoyama, H.; Yamauchi, M.; Xie, S.; Tsukuda, T. Organogold Clusters Protected by Phenylacetylene. *J. Am. Chem. Soc.* **2011**, *133*, 20123–20125.
- (20) Chakraborty, P.; Nag, A.; Chakraborty, A.; Pradeep, T. Approaching Materials with Atomic Precision Using Supramolecular Cluster Assemblies. *Acc. Chem. Res.* **2019**, *52*, 2–11.
- (21) Kang, X.; Zhu, M. Intra-cluster Growth Meets Inter-cluster Assembly: The Molecular and Supramolecular Chemistry of Atomically Precise Nanoclusters. *Coord. Chem. Rev.* **2019**, *394*, 1–38.
- (22) Nonappa; Haataja, J. S.; Timonen, J. V. I.; Malola, S.; Engelhardt, P.; Houbenov, N.; Lahtinen, M.; Häkkinen, H.; Ikkala, O. Reversible Supracolloidal Self-Assembly of Cobalt Nanoparticles to Hollow Capsids and Their Superstructures. *Angew. Chem.* **2017**, *129*, 6573–6577.
- (23) Crini, G. Review: A History of Cyclodextrins. *Chem. Rev.* **2014**, *114*, 10940–10975.
- (24) Mathew, A.; Natarajan, G.; Lehtovaara, L.; Häkkinen, H.; Kumar, R. M.; Subramanian, V.; Jaleel, A.; Pradeep, T. Supramolecular Functionalization and Concomitant Enhancement in Properties of  $\text{Au}_{25}$  Clusters. *ACS Nano* **2014**, *8*, 139–152.
- (25) Moussawi, M. A.; Leclerc-Laronze, N.; Floquet, S.; Abramov, P. A.; Sokolov, M. N.; Cordier, S.; Ponchel, A.; Monflier, E.; Bricout, H.; Landy, D.; et al. Polyoxometalate, Cationic Cluster, and  $\gamma$ -Cyclodextrin: From Primary Interactions to Supramolecular Hybrid Materials. *J. Am. Chem. Soc.* **2017**, *139*, 12793–12803.
- (26) Nag, A.; Chakraborty, P.; Paramasivam, G.; Bodiuzzaman, M.; Natarajan, G.; Pradeep, T. Isomerism in Supramolecular Adducts of Atomically Precise Nanoparticles. *J. Am. Chem. Soc.* **2018**, *140*, 13590–13593.
- (27) Chakraborty, P.; Nag, A.; Paramasivam, G.; Natarajan, G.; Pradeep, T. Fullerene-Functionalized Monolayer-Protected Silver Clusters:  $[\text{Ag}_{29}(\text{BDT})_{12}(\text{C60})_n]^{3-}$  ( $n = 1–9$ ). *ACS Nano* **2018**, *12*, 2415–2425.
- (28) Chakraborty, P.; Nag, A.; Sugi, K. S.; Ahuja, T.; Varghese, B.; Pradeep, T. Crystallization of a Supramolecular Coassembly of an Atomically Precise Nanoparticle with a Crown Ether. *ACS Mater. Lett.* **2019**, *1*, 534–540.
- (29) Kim, D.-S.; Kang, E.-S.; Baek, S.; Choo, S.-S.; Chung, Y.-H.; Lee, D.; Min, J.; Kim, T.-H. Electrochemical Detection of Dopamine Using Periodic Cylindrical Gold Nanoelectrode Arrays. *Sci. Rep.* **2018**, *8*, 14049.
- (30) Su, H.; Sun, B.; Chen, L.; Xu, Z.; Ai, S. Colorimetric Sensing of Dopamine Based on the Aggregation of Gold Nanoparticles Induced by Copper Ions. *Anal. Methods* **2012**, *4*, 3981–3986.
- (31) van der Linden, M.; Barendregt, A.; van Bunningen, A. J.; Chin, P. T. K.; Thies-Weesie, D.; de Groot, F. M. F.; Meijerink, A. Characterisation, Degradation and Regeneration of Luminescent  $\text{Ag}_{29}$  Clusters in Solution. *Nanoscale* **2016**, *8*, 19901–19909.
- (32) Baksi, A.; Bootharaju, M. S.; Chen, X.; Häkkinen, H.; Pradeep, T.  $\text{Ag}_{11}(\text{SG})_7$ : A New Cluster Identified by Mass Spectrometry and Optical Spectroscopy. *J. Phys. Chem. C* **2014**, *118*, 21722–21729.
- (33) Lopez, P.; Lara, H. H.; Mullins, S. M.; Black, D. M.; Ramsower, H. M.; Alvarez, M. M.; Williams, T. L.; Lopez-Lozano, X.; Weissker, H.-C.; García, A. P.; et al. Tetrahedral (T) Closed-Shell Cluster of 29 Silver Atoms & 12 Lipoate Ligands,  $[\text{Ag}_{29}(\text{R}-\alpha\text{-LA})_{12}]^{(3-)}$ : Antibacterial and Antifungal Activity. *ACS Appl. Nano Mater.* **2018**, *1*, 1595–1602.
- (34) Wen, D.; Liu, W.; Herrmann, A.-K.; Haubold, D.; Holzschuh, M.; Simon, F.; Eychmüller, A. Simple and Sensitive Colorimetric Detection of Dopamine Based on Assembly of Cyclodextrin-Modified Au Nanoparticles. *Small* **2016**, *12*, 2439–2442.
- (35) Govindaraju, S.; Ankireddy, S. R.; Viswanath, B.; Kim, J.; Yun, K. Fluorescent Gold Nanoclusters for Selective Detection of Dopamine in Cerebrospinal Fluid. *Sci. Rep.* **2017**, *7*, 40298.